ORIGINAL RESEARCH

Preparation of eco-friendly flame-retardant cotton fabrics based on chemical grafting and calcium chelation

Lingling Guo · Jialong Tian · Zhenming Qi ·
Yajie Zhu · Yujiao Lv · Haiyan Mao · Yujie Chen ·
Guoqiang Li · Chunxia Wang

Abstract In this study, a novel strategy is proposed to prepare eco-friendly flame-retardant cotton fabrics, where chloroacetic acid (MCA) and L-glutamic acid (L-Glu) are used as raw materials to enhance the chelation ability between carboxyl groups (-COO-) and calcium ions (Ca^{2+}). The morphological and structural characterizations of the prepared cotton fabrics indicate that the three free hydroxy groups (2, 3, 6) in the cellulose macromolecule are chemically modified to graft a large number of carboxyl groups, and Ca^{2+} ions are successfully chelated on the surface of cotton fabric. The thermal stability of cotton fabrics is greatly improved in both air and nitrogen atmosphere. The residual mass of flame-retardant cotton fabric (COT-Glu–Ca) is much higher than that of original cotton fabric, increasing from 0.03% to 5.6% in air and from 8.1% to 28.2% in N_2, respectively. At the same time, the limiting oxygen index (LOI) of COT-Glu–Ca fabric is as high as 33.6%. The prepared flame-retardant cotton fabric can undergo vertical combustion tests with a char length of only 53 mm, and afterflame and afterglow are not observed, which proves that the grafted cotton fabric had a good flame retardancy due to a series of modifications and adsorption of Ca^{2+} ions. The properties of the cotton fabric, including tensile strength, whiteness, and moisture absorption, are all retained at a satisfactory level. Overall, this study provides a promising strategy for manufacturing eco-friendly, phosphorus-free, halogen-free, and fire-resistant cotton fabrics with enhanced metal ion chelation ability.

L. Guo · J. Tian · Z. Qi · Y. Lv · H. Mao · Y. Chen ·
C. Wang (✉)
College of Textile & Clothing, Yancheng Institute
of Technology, Yancheng 224051, China
e-mail: cxwang@mail.dhu.edu.cn

Y. Zhu
Key Laboratory Integrated Regulation and Resource
Development On Shallow Lakes, Ministry of Education,
College of Environment, Hohai University,
Nanjing 210098, China

G. Li
Jiangsu Yueda Home Textile Co., Ltd, Yancheng 224005,
China

Graphical abstract
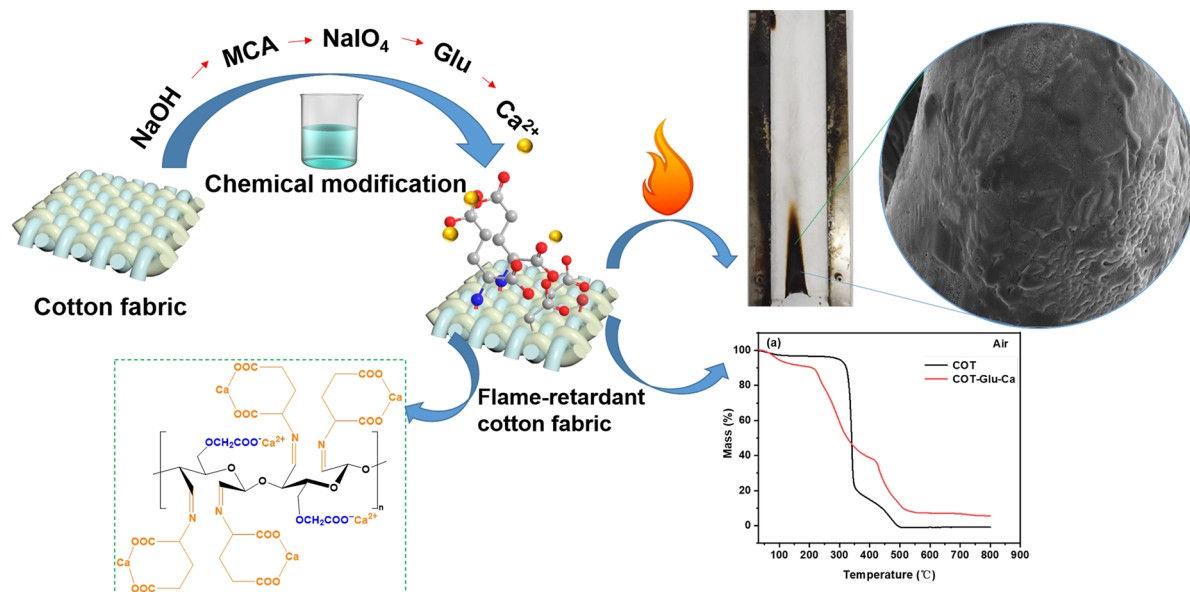
Introduction

Cotton fabrics are very popular due to their exceptional properties, such as softness, comfort, strong moisture absorbance, skin friendliness, and high breathability (Li et al. 2017; Tian et al. 2022). In fact, cotton is the most prevalent natural cellulose textile used in clothing, home furnishings, and industrial applications. However, cotton fabrics are highly flammable, with a limiting oxygen index (LOI) of 18% and an ignition temperature of only 350 °C (Rosace et al. 2017; Shariatinia et al. 2015), which is much lower than that of other common textile materials. Thus, in the event of a fire, cotton fabrics can easily ignite and burn rapidly, posing a serious threat to human life and property (Luo et al. 2020). Therefore, it is essential to apply flame retardants onto the surface of cotton fabrics to improve their fire retardancy.

Currently, several flame retardants are utilized in cotton fabrics, including halogen-, phosphorus-, nitrogen-, silicon-, and boron-based compounds, metal compounds, and collaborative flame retardants (Chen et al. 2021). Among them, phosphorus-containing flame retardants, such as Proban® and Pyrovatex CP®, are widely used due to their dual functionality of flame retardancy and plasticization, high efficiency, low toxicity, less smoke, halogen-free or low halogen content, and high thermal stability. However, phosphorus-based flame retardants block the hydroxy groups in cellulose macromolecules, which significantly reduces other textile properties such as gas permeability, comfort, flexibility, and so on. Additionally, the excessive use of organophosphate flame retardants can lead to environmental pollution, threatening human health (Wei et al. 2015; Yang et al. 2021). Therefore, it is imperative to establish an effective method for manufacturing eco-friendly flame-retardant cotton fabrics.

Notably, intrinsically flame-retardant alginate fibers, such as sodium alginate, zinc alginate, barium alginate, copper alginate and calcium alginate fibers (Liu et al. 2015b; Lv et al. 2012), do not contain phosphorus and halogens and have impressive flame retardancy. Alginate, which is composed of two repeating monomeric units: α-1, 4-L-guluronate (G)

and β-1, 4-D-mannuronate (M) (Chen et al. 2012), is a natural non-toxic copolymer (Agulhon et al. 2012) and has similar macromolecular structure as cotton cellulose (French 2017). Alginate fibers are produced through the wet spinning of sodium alginate into a coagulation bath of various metal ions, which may form a specific network structure between uronic acid residues and metal ions. Zhang et al. (2012) investigated the effect of divalent metal ions, including Zn^{2+}, Cu^{2+}, and Ba^{2+}, on the flame retardancy and pyrolysis products of alginate fibers. They found that the addition of these ions enhanced the char formation and flame retardancy of alginate fibers. Liu et al. (2016) examined the effect of reaction time on the flame retardancy and thermal stability of zinc alginate film, and the results revealed that zinc ions had a catalytic effect during the pyrolysis process, favoring the decarboxylation of alginate, thereby accelerating the thermal degradation process of alginate and improving the flame retardancy of alginate.

Kabir et al. (2020) presented a review of the alginate/polymer-based materials as flame retardants, focusing on their synthesis, structure, properties, and applications. It was noted that the thermal stability of alginates can be enhanced by crosslinking using suitable intercalating metals and more thermally stable graft copolymers. Metal ions have also been introduced into other textile materials. Qu et al. (2022) prepared a biomass-based flame retardant using bio-material glycine and aspartic acid as raw materials. Glycine and aspartic acid were converted into sodium carboxylates (glycine-Na and aspartate-Na), which were then grafted onto the molecular chain of lyocell cellulose by formaldehyde to prepare flame-retardant lyocell fabrics. The modified fabrics showed self-extinguishing characteristics and formed a greater amount of char residue containing Na_2CO_3 during combustion. Zhang et al. (2021) developed an innovative eco-friendly biomass-based coating using tannins (TA), tartaric acid (TE), and Fe^{2+} to endow cotton fabrics with excellent flame retardancy. The treated samples exhibited a LOI value of 27%. Therefore, metal ions can lower the fabric's decomposition temperature and have a catalytic effect, improving the combustion performance of the textile material.

Herein, inspired by the alginate fibers, a novel eco-friendly flame-retardant is prepared for cotton fabrics using chloroacetic acid (MCA) and L-glutamic acid (L-Glu) as raw materials. Specifically, MCA is grafted onto C_6 hydroxy group of cotton fabric to form carboxymethyl cellulose (COT-CMC). Subsequently, the C_2–C_3 bond of cellulose is oxidized by sodium periodate ($NaIO_4$) to form dialdehyde carboxymethyl fabric (COT–DCMC), and then L-Glu is cross-linked with the aldehyde groups to form fabric with polycarboxylic group (COT-Glu) to introduce a large number of carboxyl groups, which further absorb Ca^{2+} ions to form a protective network structure on the cotton fabric. The proposed modification strategy forms more rigid metal oxides/carbides as a non-flammable char residue barrier after heating, and the resultant cotton fabric is eco-friendly, non-toxic, halogen-free, phosphorus-free, and fire-resistant. The morphological, structural, and mechanical properties of the fabric are analyzed by a variety of techniques, such as Fourier-transform infrared (FTIR) spectroscopy, X-ray photoelectron spectroscopy (XPS), X-ray diffraction (XRD), scanning electron microscopy (SEM), energy dispersive X-ray spectroscopy (EDS), and thermogravimetric/differential thermogravimetric (TG/DTG) analysis.

Experimental

Materials

Sodium hydroxide (NaOH) was obtained from Jiangsu Tongsheng Chemical Reagent Co., Ltd. (Yixing, China). MCA ($ClCH_2COOH$) was procured from Shandong West Asia Chemical Industry Co., Ltd. (Shandong, China). Sodium Periodate ($NaIO_4$) was obtained from Shanghai Shanpu Chemical Co., Ltd. (Shanghai, China). L-Glu ($C_5H_9NO_4$) was bought from Bide Pharmatech Ltd. (Shanghai, China). Glacial acetic acid (CH_3COOH) was purchased from Sinopharm Chemical Reagents Co., Ltd. (Shanghai, China). Glycerol ($C_3H_8O_3$) and anhydrous calcium chloride ($CaCl_2$) were procured from Sinopharm Chemical Reagents Co., Ltd. (Shanghai, China). All the chemical reagents were analytically pure and were used without further purification. Cotton fabric (linear density: 20 tex×20 tex; fabric density: 300 yarns/10 cm×300 yarns/10 cm; weight: 112 g/m^2; plain weave) was obtained from the Shanghai Textile
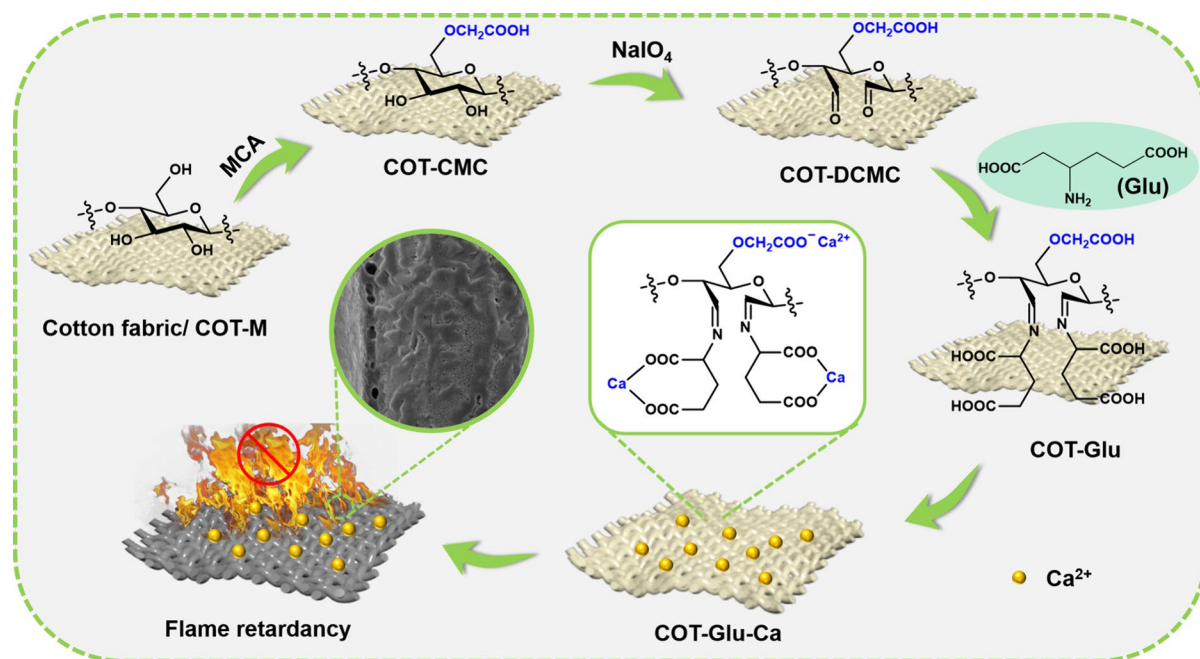
Scheme 1 Schematic illustration of the modification process of flame-retardant cotton fabrics

Industry Technical Supervision Institute (Shanghai, China).

Grafting modification and Ca^{2+} chelation of cotton fabrics

The modification and Ca^{2+} ion chelation processes of cotton fabric are illustrated in Scheme 1. Firstly, the cotton fabric (300 mm × 89 mm) was immersed in NaOH solution (24 wt%, bath ratio: 1:25) under continuous stirring for 10 min at room temperature. Excessive NaOH was decomposed by 24 wt% acetic acid solution. Subsequently, the sample was stirred for 10 min, washed, and then dried in an oven at 60 ℃ to synthesize alkali-treated cotton fabric (COT-M). Secondly, the COT-M was immersed in 25 wt% aqueous MCA solution under continuous stirring at 40 °C for 4 h, which was then washed and dried at 60 °C for 2 h under vacuum to obtain carboxymethylated cotton fabric (COT-CMC). Thirdly, the COT-CMC was continuously oxidized by 0.2 mol/L sodium periodate solution under vigorous stirring in dark at 40 °C for 1 h and then immersed in 0.1 mol/L glycerol solution (bath ratio of 1:17) under stirring at room temperature for 30 min, followed by drying to obtain an oxidation

product, named COT-DCMC. Subsequently, the COT-DCMC sample was immersed into 50 mmol/L L-Glu solution for 1 h, followed by washing and drying to obtain the grafted fabric (COT-Glu). Finally, the COT-Glu fabric was soaked in 200 g/L $CaCl_2$ solution for 1 h of chelation reaction and then washed with deionized water to remove unreacted $CaCl_2$. After drying, the flame-retardant cotton fabric (COT-Glu–Ca) was obtained. The weight gain (WG) of the flame-retardant sample was calculated as follows:

$$WG\ (\%) = (m_{FR} - m_0)/m_0 \times 100$$

where m_0 and m_{FR} represent the weight of the cotton fabric before and after the flame-retardant treatment, respectively.

Characterization

The chemical structure and elemental composition of the modified cotton fabric were examined by FTIR spectroscopy (NEXUF-670 FTIR spectrometer, Nicolet, USA) and XPS (ESCALAB 250Xi spectrometer, Thermo Fisher, UK). The crystal structure of the cotton fabric at each modification step was

investigated using XRD (X'Pert[3] Powder X-ray diffractometer, PANalytical, Holland) with Cu Ka radiation ($\lambda = 0.15418$ nm) over a 2θ (Bragg angle) range of 10–80° with a scan step size of 0.026°. The surface morphology of the cotton fabric at each modification step and the residue after vertical combustion were observed by SEM (Nova NanoSEM 450 field emission scanning electron microscope, FEI, USA) with an acceleration voltage of 5 kV, while the elements on the surfaces of samples were analyzed by EDS (Aztec X-MaxN80 energy spectrometer, Oxford, UK) equipped in the SEM apparatus. The samples were cut into a size of 5 mm×5 mm and glued to the special stage with a conductive adhesive, and gold sputter coating was performed for 45 s before the examination. The thermal stability of the samples were examined by TG analysis (STA6000 simultaneous thermal analyzer, Perkin Elmer, USA). The temperature range was 40–800 ℃ in N_2 and air, with a heating rate of 10 ℃/min.

The flame resistance and durability of cotton fabric were evaluated by LOI and vertical combustion tests. The LOI of cotton fabric was measured by HC-2 oxygen index tester (Ruixinjie Instrument, China). The size of the cotton fabric was 150 mm×50 mm. The LOI test was carried out by adjusting the O_2 flow rate. The vertical combustion test was performed using a YG(B)815D-I fabric flame resistance tester (Darong Textile Standard Instrument, Wenzhou, China). The size of the cotton fabric was 89 mm×300 mm. The tensile strength of cotton fabric was measured using a YG(B) 026D-250 strength tester (Darong Textile Standard Instrument, Wenzhou, China) under normal conditions. The sample was 200 mm (warp)×50 mm (weft), tested along the warp direction three times. The whiteness of cotton fabric was tested on a WSD-3 automatic whiteness meter (Kangguang Instrument, China). The wettability of samples before and after modification was evaluated by static contact angle measurements on a JC2000D3 tester (Zhongchen Digital Technic Equipment Co., Ltd, Shanghai, China). According to the AATCC 61–2013 standard, the durability test was performed by a SW-12AII washing fastness testing instrument (Darong Textile Standard Instrument, Wenzhou, China). The fire-proof cotton fabric was repeatedly washed in a 500 mL rotating closed stainless-steel canister containing 0.15 wt% soap powder at 49 ℃ (bath ratio of 1:50, 15 min for a cycle). The white soap powder was manufactured from the Shanghai Textile Industry Technical Supervision Institute, China.

Result and discussion

FTIR spectroscopic analysis

The FTIR spectra of the samples at each modification step are shown in Fig. 1. Compared to the control cotton sample (COT), the peak around 3336 cm^{-1}, which is attributed to the stretching vibration of the hydrogen bonded –OH group (Li et al. 2017), becomes
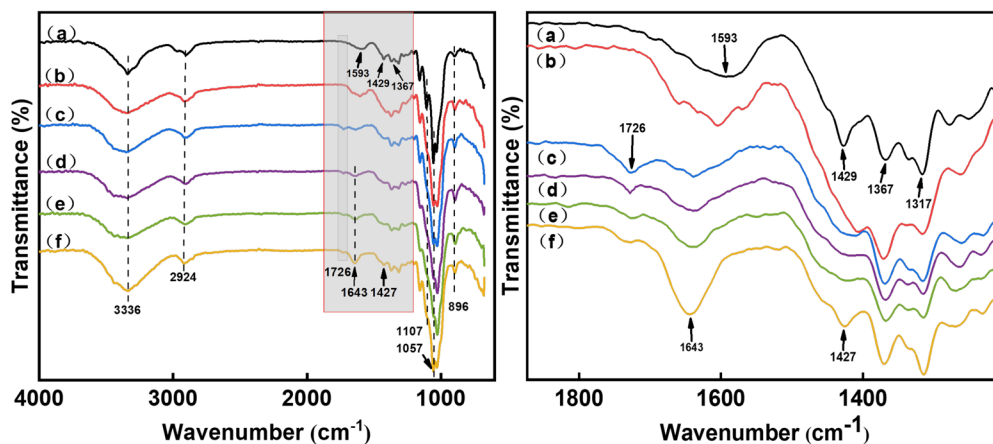
Fig. 1 FTIR spectra of different samples (left) and their local magnifications (right): (a) COT, (b) COT-M, (c) COT-CMC, (d) COT-DCMC, (e) COT-Glu, and (f) COT-Glu–Ca

broader and stronger in cellulose, indicating that the number of free hydroxy groups on the cotton cellulose gradually increase through the chemical reaction with MCA and L-Glu. The peaks at approximately 1429 and 1367 cm^{-1}, which are assigned to CH$_2$ deformation vibration and C–H bending vibration (Castellano et al. 2019; Li et al. 2017), are significantly changed (Fig. 1, curve (b)), suggesting that the crystallinity of cellulose is reduced after treatment with NaOH (Abidi, 2014). Meanwhile, the peaks near 1057 and 1107 cm^{-1}, which are attributed to C–O–C stretching vibrations (Lin et al. 2019), are much weaker than those of the pristine fabric, indicating that the carbon background is destroyed to a certain extent.

After reaction with MCA, a new peak appears at approximately 1726 cm^{-1}, which corresponds to the C=O stretching vibration of carbonyl groups (Liu et al. 2016; Shariatinia et al. 2015), confirming that the MCA monomers are grafted onto the macromolecules of cotton fabric. Nevertheless, the intensity of the peak ascribed to aldehydic carbonyl groups significantly decreases in the spectrum of COT-DCMC (Fig. 1, curve (d)). This is because the band around 896 cm^{-1} is assigned to the formation of hemiacetal/acetal bonds between the aldehyde groups and adjacent hydroxy groups (Kang, 2002; Liu et al. 2017; Zhang et al. 2020). These results show that the aldehyde groups are introduced into the structure by selective periodate oxidation. Compared to curve (d), the characteristic peak corresponding to the aldehyde group becomes much weaker in curve (e). Further, the two peaks near 1643 and 1427 cm^{-1} are ascribed to the asymmetric stretching vibration and symmetric stretching vibration of COO–groups (Leal et al. 2008; Li et al. 2015; Liu et al. 2015a), respectively. Therefore, it can be inferred that aldehyde groups react with amine groups of L-Glu, and the carboxyl groups in COT-Glu exist in the form of carboxylates with higher intensity. Furthermore, the peak at 1645 cm^{-1} is assigned to the amide I band (C=N stretching vibration) (Yue et al. 2014), which overlaps with the asymmetric stretching vibration peak of COO–groups. The absorption bands around 1645, 1427, and 1052 cm^{-1} are remarkably enhanced in curve (f) as compared to those in curve (e), which further verifies that a large number of carboxylic groups are introduced into the cotton fabric, moreover those undergo the chelation reaction with Ca^{2+} ions (Li et al. 2015; Wang et al. 2019b).

XPS analysis

To further verify the surface chemical composition of flame-retardant cotton fabric and the chelating effect of Ca^{2+} with carboxyl group in the cellulose, the wide-scan XPS spectra of the samples at each modification step were obtained. All five samples show the presence of C and O (see wide-scan spectra in Fig. 2), while new peaks of N 1 s and N 1s, Ca 2p are observed in the wide-scan XPS spectra of COT-Glu and COT-Glu–Ca, respectively. The high-resolution C1s spectra of the five samples are also shown in Fig. 2.

For the COT-M sample, the three peaks at 284.6, 286.4, and 287.7 eV are assigned to the C–C/C–H, C–OH, and O–C–O bonds, respectively (Castellano et al. 2019; Miao et al. 2021). However, the peak shapes in the C 1s spectrum of COT-CMC (Fig. 2b) are significantly different from that of the COT-M sample (Fig. 2c). A new peak at 288.9 eV assigned to ester bonds (-COO) is detected (Liu et al. 2022), and the C–OH peak becomes much higher and stronger, indicating that a larger amount of MCA is grafted on the alkali-treated cotton fabric. Further, the C–OH ratio in the COT-DCMC sample becomes significantly smaller than that in the COT-M and COT-CMC samples, and the peak at 287.1 eV corresponding to the carbon atoms in O-C-O or C=O after oxidation slightly shifts (0.6 eV) toward lower binding energy, suggesting that the hydroxy groups at the C$_2$-C$_3$ position are oxidized by NaIO$_4$ to form aldehyde groups. After grafting with L-Glu, Fig. 2d), the two new peaks observed at 285.6 eV and 284.0 eV: one is associated with the inherent C–N bond in L-Glu (Wang et al. 2019a), and the other is related to the Schiff base reaction between the amino and aldehyde groups to generate C=N, thereby achieving the expected design. After chelation with Ca^{2+} ions, the peaks of C–OH, C–N, and C=O/C–O–C become significantly weaker, which indicates that a calcium carboxylate (–COOCa$^{1/2}$) network is formed on the surface of cotton fabric.

In the high-resolution N 1s spectrum (Fig. 3a), the peaks at 399.4 eV and 400.4 eV are attributed to C–N (Liu et al. 2022; Qu, 2022) and C=N (Xiao et al. 2021), respectively. Meanwhile, the peaks related to –NH$_2$ group are not detected, indicating that the –NH$_2$ group reacts with the -C=O group to form new chemical bonds and is completely consumed. After
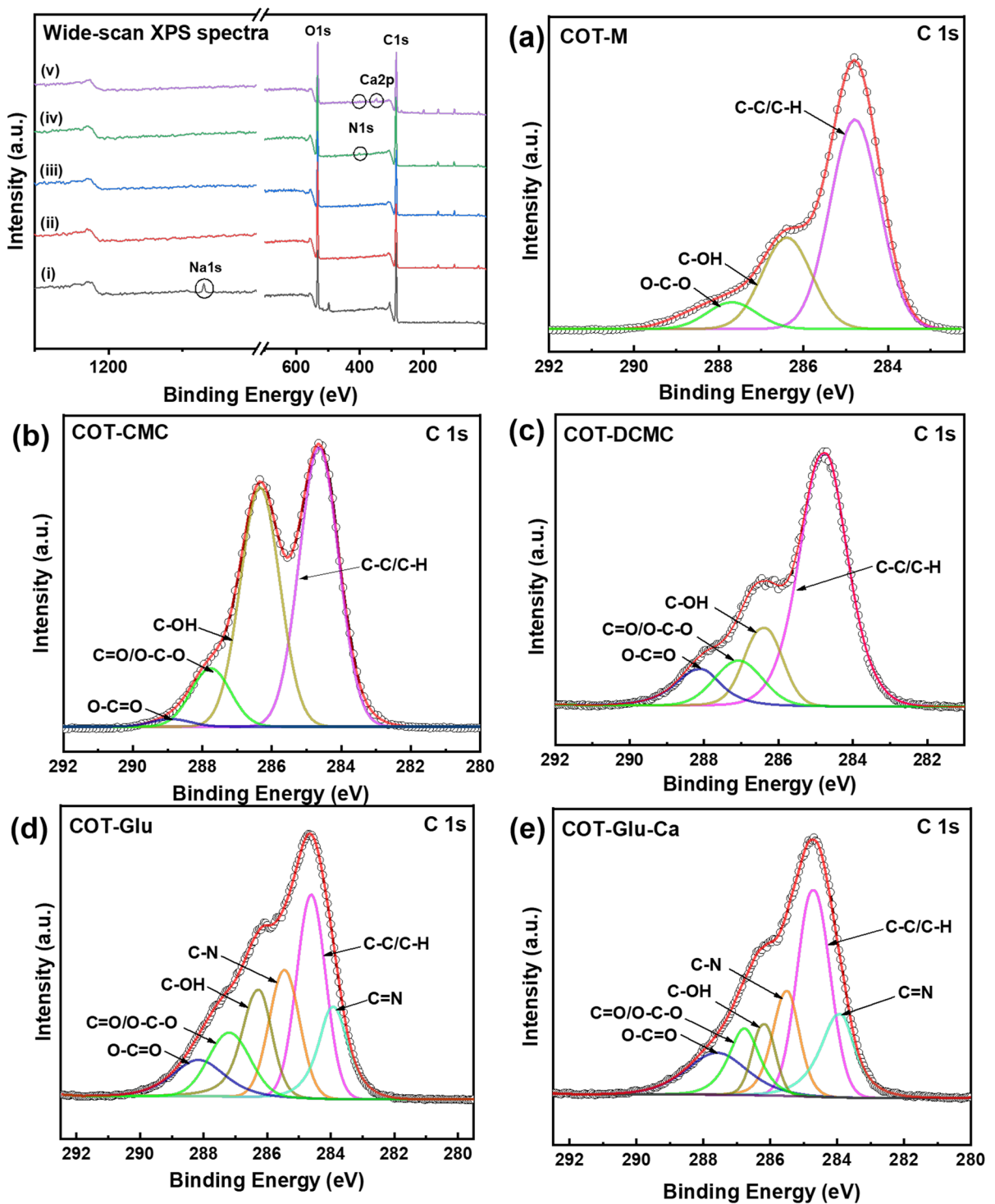
Fig. 2 Wide-scan XPS spectra of the samples at each treatment step: (i) COT-M, (ii) COT-CMC, (iii) COT-DCMC, (iv) COT-Glu, and (v) COT-Glu–Ca. Deconvoluted high-resolution C1s XPS spectra of: (**a**) COT-M, (**b**) COT-CMC, (**c**) COT-DCMC, (**d**) COT-Glu, and (**e**) COT-Glu–Ca
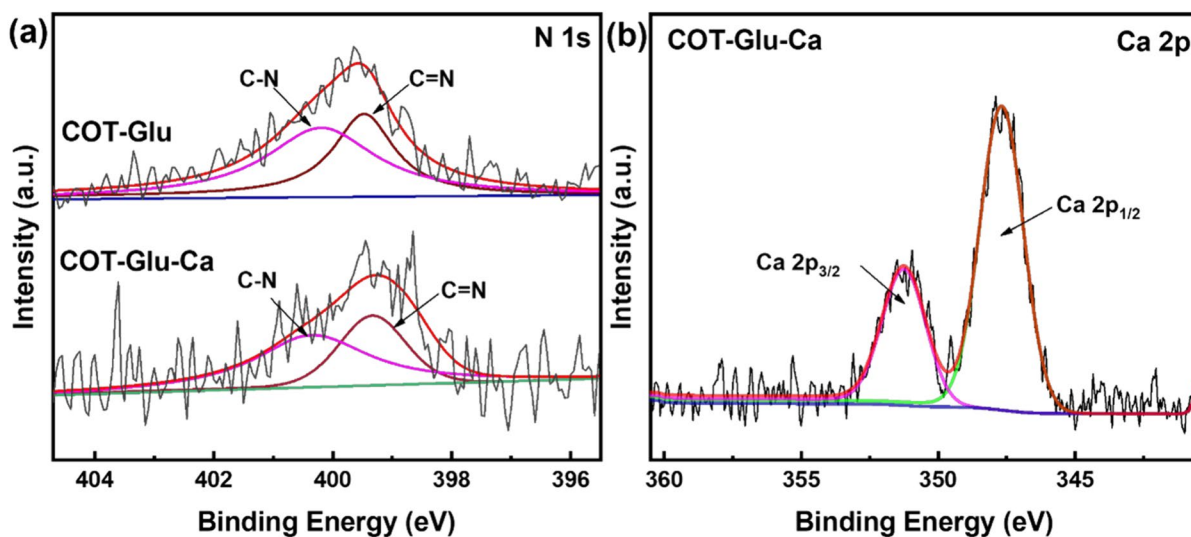
Fig. 3 Deconvoluted high-resolution N 1s and Ca 2p XPS spectra
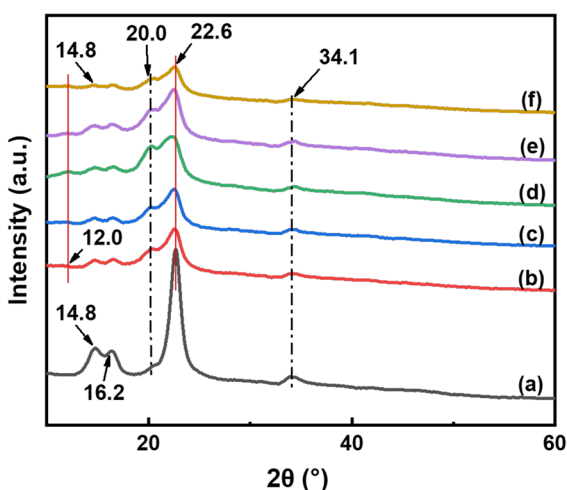

Fig. 4 XRD patterns: (**a**) COT, (**b**) COT-M, (**c**) COT-CMC, (**d**) COT-DCMC, (**e**) COT-Glu, and (**f**) COT-Glu–Ca

chelation with Ca^{2+} ions (Fig. 3a), the intensity and width of the peak related to the –C–N bond slightly increase, while the peaks corresponding to –C–N and –C=N bonds are slightly shifted toward higher binding energy, indicating that Ca^{2+} ions are adsorbed on the treated samples by carboxyl groups. Moreover, the Ca 2p spectrum shows doublet peaks of Ca $2p_{3/2}$ at 347.7 eV and Ca $2p_{1/2}$ at 351.3 eV, which is consistent with an earlier study (Wang et al. 2019b). Overall, the XPS results indicate that –COO- successfully

coordinates with the Ca^{2+} ions adsorbed on the surface of the modified cotton fabric through its carboxylic oxygen atoms.

XRD analysis

Figure 4 shows the XRD patterns of COT, COT-M, COT-CMC, COT-DCMC, COT-Glu, and COT-Glu–Ca samples. The diffraction peaks of pristine cotton cellulose (curve (a)) are approximately located at $2\theta = 14.8°$, $16.2°$, $22.6°$, and $34.1°$, which correspond to the reflections from the (1–10), (110), (200), and (004) crystallographic planes of cellulose I, respectively (Lu et al. 2018; Xing et al. 2020). For alkali-treated sample, the strengths of the peaks at $14.8°$, $16.2°$ and $22.6°$ dramatically decrease. The peak around $22.6°$ for cellulose II plane (020) is close to that for cellulose I plane (200) (Kafle et al. 2014). Meanwhile, the diffraction peak around $20°$ for cellulose II (110) plane is becoming increasingly apparent due to the varying amounts of preferred orientation (French 2014). Furthermore, a peak appears around $12.0°$, which corresponds to the cellulose II plane (1–10) (Jin et al. 2016). Therefore, the structure for cotton fabric modified with 24 wt% NaOH solution is partially transformed from cellulose I to cellulose II. Compared to curve (b), the peaks at $22.6°$ in curves (c~e) have slightly shifted, which may be that the carboxylate and aldehyde groups are introduced to the

Fig. 5 SEM images of cotton fabric during grafting and chelation: (**a**) COT × 5000, (**b**) COT-M × 5000, (**c**) COT-CMC × 5000, (**d**) COT-DCMC × 5000, (**e**) COT- Glu × 5000, (**f**) COT-Glu–Ca × 5000, (**g**) Char layer of COTGlu–Ca × 500 and (**h**) Char layer of COT-Glu–Ca × 5000
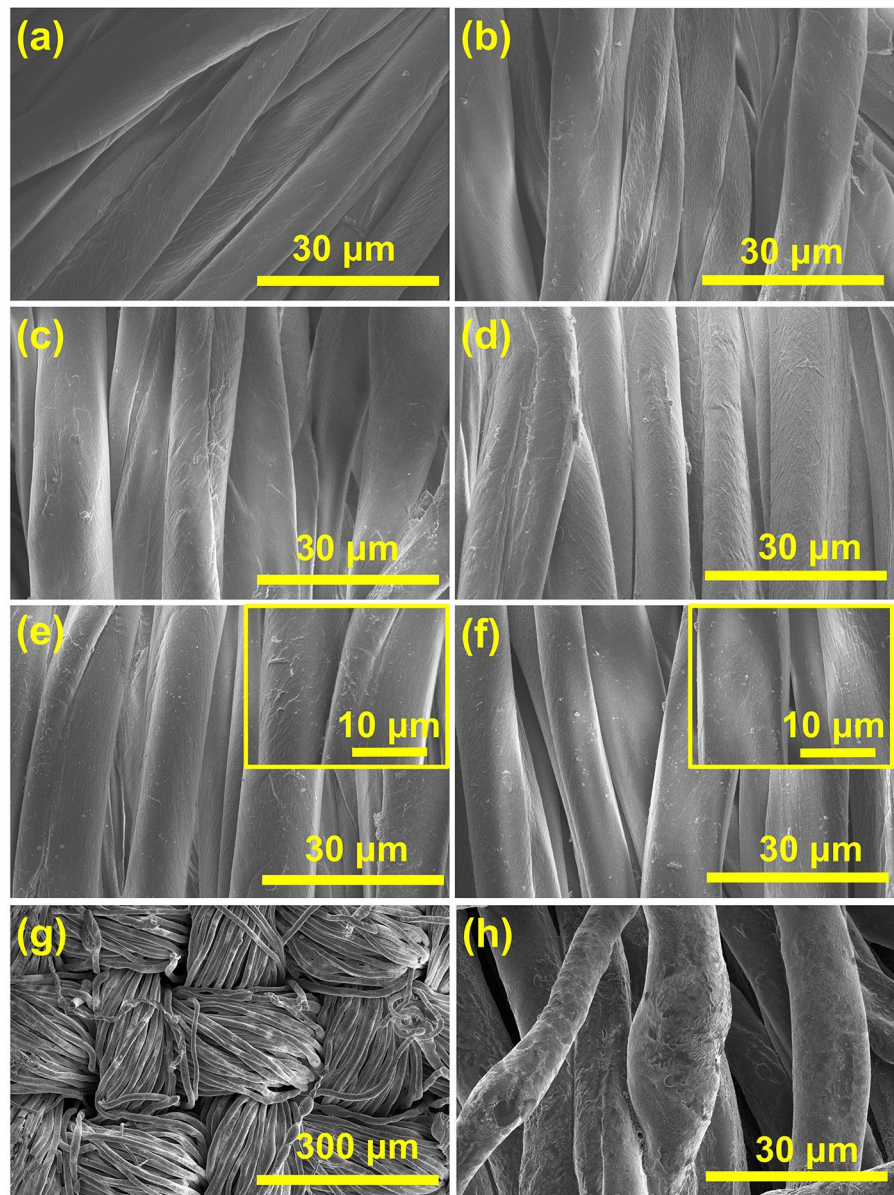
crystal surface of cellulose II (Mendoza et al. 2019). Moreover, the relative intensity of the peak in curve (f) shows almost no change compared to curve (e). It may be inferred that interaction between Ca^{2+} ions and COO- only occurs on the surface of COT-Glu (Hong et al. 2016; Pinto et al. 2012). These results could further demonstrate the successful modification of the cotton fabric.

SEM and EDS analysis

The morphology of cotton fibers is examined by SEM images, and the evolution of the fabric from initial form to final char residue is shown in Fig. 5. The surface of the original cotton fabric is applanate and smooth, and no other substances are found. After alkaline treatment, the fiber surface of the cotton fabric becomes smoother and plump. The surface morphology of cotton slightly changes and a thin film appears after MCA grafting and $NaIO_4$ treatment.
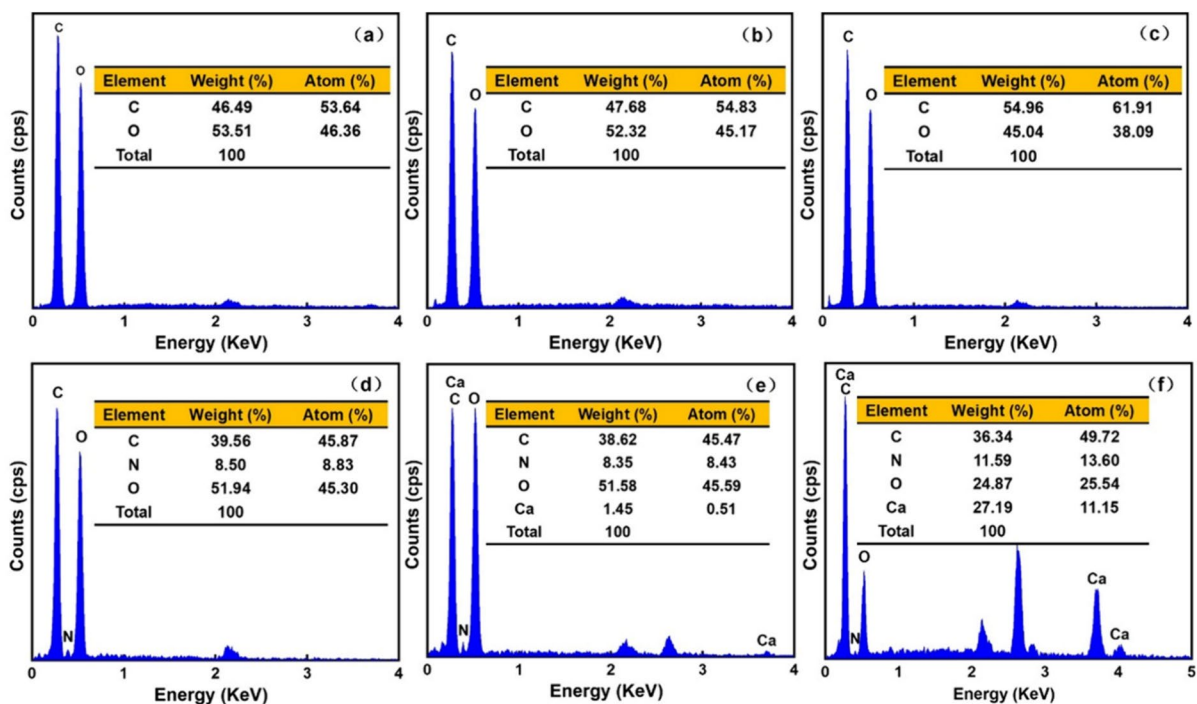
Fig. 6 EDS analysis of cotton fabrics: (**a**) COT, (**b**) COT-CMC, (**c**) COT-DCMC, (**d**) COT-Glu, (**e**) COT-Glu–Ca,and (**f**) carbon residues of COT-Glu–Ca

After L-Glu and $CaCl_2$ treatment, the surface of cotton fabric becomes rough, and tiny white particles are observed, indicating the successful grafting of L-Glu on the cellulose macromolecule and the effective adsorption of Ca^{2+} ions on the surface of cotton fabric. Combined with XPS and FTIR spectroscopic analysis, it is confirmed that the cotton fabric is effectively modified and chelated.

The chemical compositions of cotton fabrics before and after treatment are analyzed by EDS. The atomic weight ratios of cotton fabrics obtained by EDS are shown in Fig. 6. The COT-CMC and COT-DCMC fabrics only contain C and O elements, mainly from cotton fabric and MCA, while the COT-Glu samples contain not only C and O but also N from L-Glu, which confirms that L-Glu is successfully grafted on the cotton fabric. Additionally, Ca(II), with a weight percentage of 10.14%, is detected in COT-Glu–Ca, illustrating that Ca^{2+} ions are adsorbed on the surface of cotton fabric. As shown in Fig. 6e and f, the calcium side peak near 0.3 keV overlaps with the C peaks. For the char layer, the atomic weight ratio of O decreases and that of N and Ca^{2+} increases,

suggesting that Ca^{2+} ions play an important role in the condensed-phase flame retardants. A protective film of calcium carbonate is formed by the oxidation of calcium ions, which helps in isolating the air, blocking heat, and mass transport during combustion. The atomic percentages of C and O in the carbon layer are significantly reduced after combustion, which is ascribed to the generation of a large amount of non-flammable gases (H_2O, CO_2, etc.) during combustion. The increase in the atomic percentage of Ca^{2+} in the carbon layer (from 0.51 to 11.15 wt%) is also attributed to the enhanced condensed-phase flame retardant effect, which may have been caused by the thermal decomposition product $-COOCa^{1/2}$.

Thermal stability analysis

The TG and DTG curves of the original and final treated cotton fabrics in air and N_2 are presented in Fig. 7, and the relevant data are listed in Table 1. The final modified sample (COT-Glu–Ca) shows three weight loss stages in air. The first weight loss stage is in the range of 43.0–167.0 °C with 8.7% weight
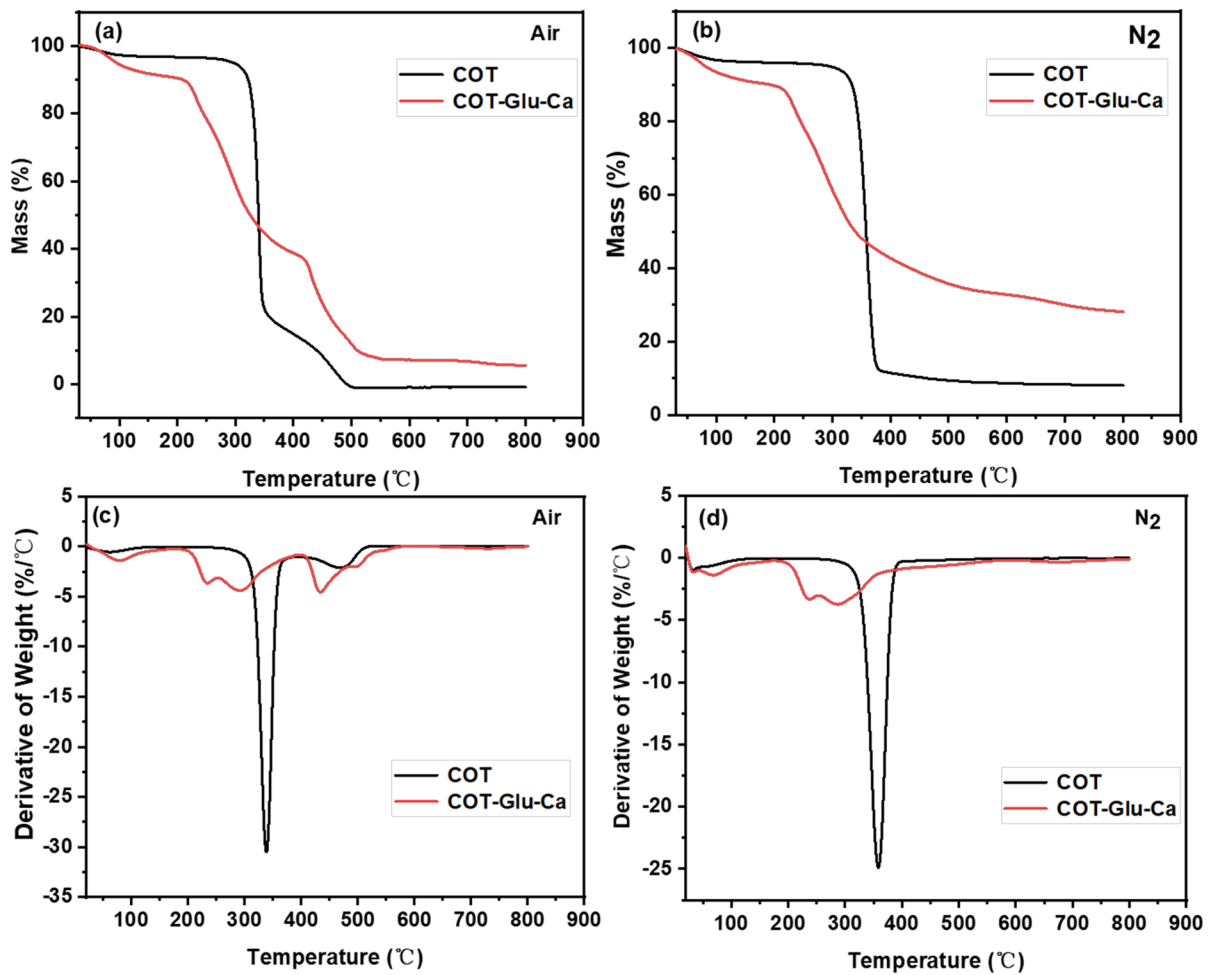
Fig. 7 TG and DTG curves of raw cotton sample (COT) and final treated cotton fabric (COT-Glu–Ca): (**a**) TG in air, (**b**) TG in N_2, (**c**) DTG in air, and (**d**) DTG in N_2

Table 1 TG data of control cotton fabric (COT) and modified cotton fabric (COT-Glu-Ga) in air and N_2

Atmosphere	Sample	T_{onset} (℃)	T_{max} (℃)	R_{max} (%/min)	Residual mass at 800 ℃ (wt%)
Air	COT	314.9	339.4	30.4	0.03
	COT-Glu–Ga	221.5	291.3	4.4	5.6
N_2	COT	325.1	358.3	24.9	8.1
	COT-Glu–Ga	217.4	287.8	3.7	28.2

loss, which is related to the evaporation of water absorbed onto the cotton fabric. The second step, in the range of 221.5–416.6 °C, shows rapid pyrolysis with the maximum weight loss rate (Rmax) of 4.4% at 291.3 °C, which is much lower than the Rmax of 30.4% for COT at 339.4 °C. This is ascribed to the decarboxylation, dehydration, and glycosidic bond breaking of modified cotton fabric (Hou et al. 2018; Liu et al. 2016), which result in the formation of intermediate products, accompanied by the release of H_2O and CO_2. The last stage is in the range of 416.6–567.0 °C. This stage includes the further

Fig. 8 Vertical combustion process of four types of fabric at different times: (**a**) COT, (**b**) fire-proof cotton fabric (COT-Glu–Ca), (**c**) fire-proof cotton fabric COT-Glu–Ca after five washing cycles, (**d**) washed and re-chelated COT-Glu–Ca
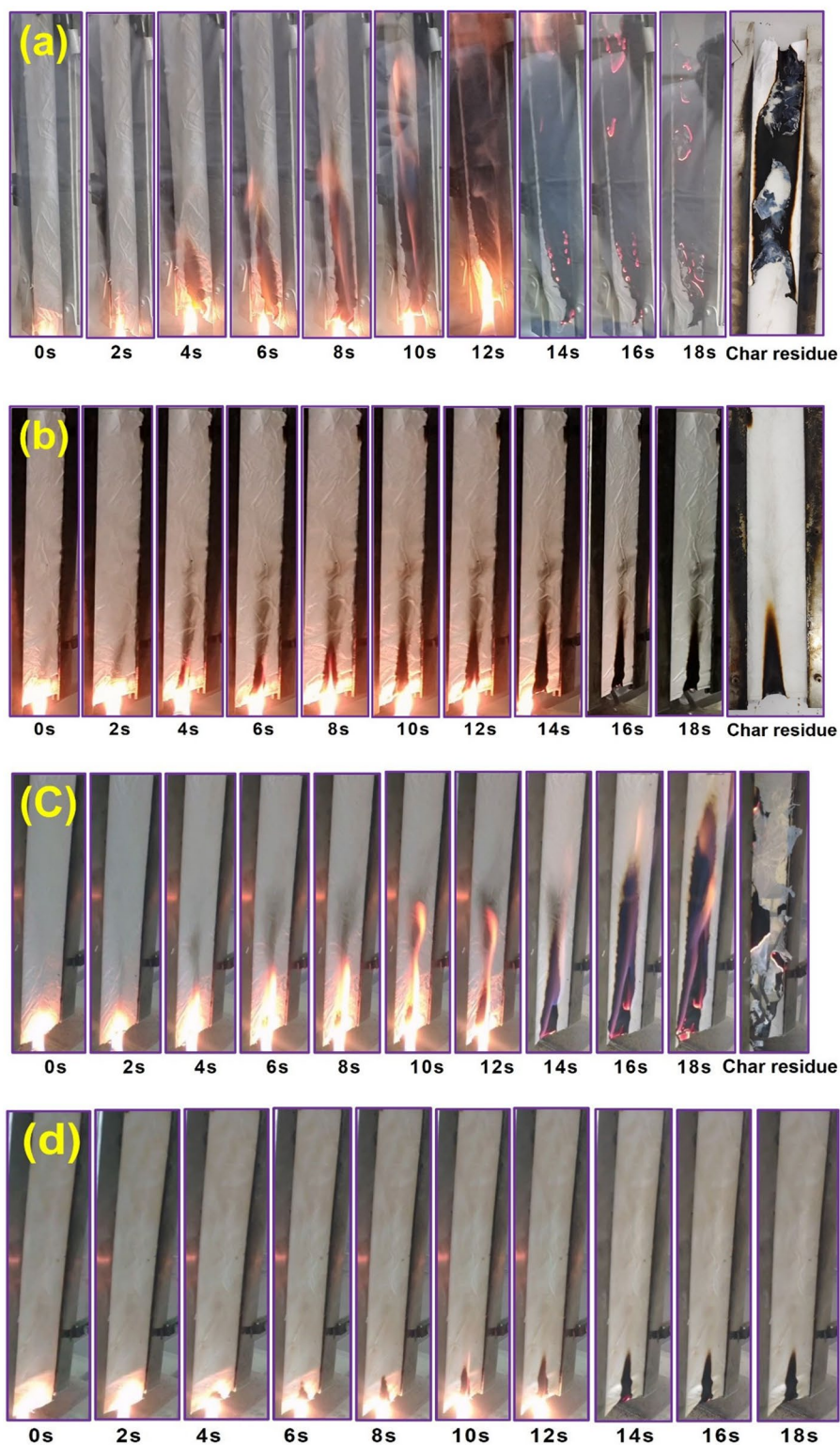
Table 2 LOI and vertical combustion characteristics of four types of fabrics in air

Sample	LOI (%)	Afterflame time (s)	Afterglow time (s)	Char length (cm)
COT	17.8	3.8	7.5	≥ 30
COT-Glu–Ca	33.6	0	0	5.3
COT-Glu–Ca washed in 5 cycles	20.9	5.2	42.9	≥ 30
Washed and re-chelated COT-Glu–Ca	31.7	0	3.2	5.9

decomposition of intermediate products and the formation of calcium oxide and stable char, which attach to the fabric surface as a protective layer. At 800 °C, the residual carbon content is 5.6 wt% compared to the almost zero content for COT. Obviously, the onset temperature of thermal decomposition (T_{onset}) of COT-Glu–Ca is nearly 95 °C lower than that of COT fabric because the calcium ions can catalyze the degradation of modified cotton fabrics at lower temperatures (below 200 °C) (Liu et al. 2014).

In N_2, the thermal decomposition process of cotton fabrics before and after flame retardant treatment shows only one major weight loss stage, except loss of adsorbed water. The maximum decomposition temperature (T_{max}) of COT-Glu–Ca is 270.5 °C, which is much lower than that of COT (358.3 °C). This prominent decrease is due to the introduction of carboxylic acid groups that cause the fibers to undergo thermal decomposition reactions such as decarboxylation in advance. In addition, it is clear from Fig. 7 and Table 2 that in N_2 atmosphere, the carbon residue of the COT-Glu–Ca sample is 28.2 wt.%, which is 248.1% higher than that of the COT fabric (8.1 wt.%). Meanwhile, the carbon residue content of the COT-Glu–Ca sample in N_2 is remarkably higher than that in air because the thermal oxidation of cotton fabric in N_2 atmosphere is inhibited.

In summary, the difference in the thermal decomposition properties between COT and COT-Glu–Ca is obvious, and COT-Glu–Ca has a lower thermal degradation temperature, a smaller maximum weight loss rate, and a higher amount of carbon residue. These phenomena prove that the introduction of carboxyl and calcium ions into the cellulose molecules can catalyze the formation of more char residue to inhibit the combustion of fibers in condensed phase. Therefore, the thermal stability and flame retardancy of cotton fabric are distinctly improved.

Flame resistance analysis

The vertical combustion process and LOI of COT, COT-Glu–Ca, COT-Glu–Ca after five washing cycles, and washed and re-chelated COT-Glu–Ca are shown in Fig. 8 and Table 2. It can be seen that the combustion characteristics of the four samples are significantly different. The control cotton fabric (COT) burns violently, rapidly, and completely, leaving a lot of loose ash, while the modified fabric (COT-Glu–Ca) does not burn obviously and forms a complete char layer after combustion. The vertical combustion effect of COT-Glu–Ca dramatically increases in comparison with the original cotton fabric, which is also reflected in the different images of the char layer and the decrease in char length, afterflame time, and afterglow time. In other words, the synthesized flame-retardant cotton fabric could undergo vertical combustion tests. Moreover, the char length is only 53 mm, and smoke is not produced. Therefore, it can be inferred that the modified cotton fabric with the specific egg-box structure formed by the chelation between several $–COO^-$ and Ca^{2+} ions served as the protective layer to prevent the heat from entering the inner fibers, endowing the modified cotton fabric with outstanding flame retardancy. Further, the flame retardancy of the fabric after washing is investigated. After five cycles of washing, the COT-Glu–Ca fabric burns slowly and does not form a complete char layer during combustion. However, if the washed COT-Glu–Ca is chelated with Ca^{2+} ions again, the fabric regains excellent flame retardant properties. This further proves that the cotton fabric grafted through a series of modifications and Ca^{2+} crosslinking has a good flame retardant effect.

It can be seen in Table 2 that the LOI of COT-Glu–Ca reaches 33.6%, which is 15.8% higher than

that of the original cotton. However, the LOI of COT-Glu–Ca after five washing cycles decreases to 20.9%, while that of washed and re-chelated COT-Glu–Ca recovers to 31.7%, indicating its excellent and recoverable flame resistance.

The Ca^{2+} ions on the fiber surface can react with the released CO_2 at high temperature to generate $CaCO_3$/CaO, which covers the surface of the burning fabric, establishing an effective barrier between the condensed phase and the fire source. As shown in the SEM images, a thick layer of solid residues is formed, which prevents the transmission of heat and oxygen to achieve flame retardancy (Liu et al. 2014; Zhang et al. 2022). At the same time, the decomposition of $CaCO_3$ absorbs a lot of heat from the surrounding environment to reduce the temperature on the fiber surface, and noncombustible gases such as CO_2 and NH_3 are produced due to the presence of N and C, which dilutes O_2 required for combustion. Besides, Ca^{2+} ions can catalyze the decarboxylation of the fabric and promote the formation of char layer, thereby protecting the internal fibers. The calcium ions and carboxyl groups play a flame retardant role in the condensed phase, greatly improving the flame retardancy of the cotton fabrics. Notably, Kabir et al. (2020) reported that higher bond energies typically lead to increased char formation due to

the better preservation of the molecular structure, so carbon–nitrogen double bonds (C=N) are preferable for char formation to improve the flame retardancy of flammable materials.

Tensile strength test, Whiteness, and Hydrophilicity

The tensile properties of cotton fabrics are also tested to investigate the effect of modification on the mechanical properties, and the results are shown in Table 3. The breaking strength of the original cotton in the warp direction is 368.4 N, which increases by 17.59% after treatment with 24 wt% NaOH solution. When cotton is grafted with MCA, the tensile strength increases to 466.8 N. This is because the macromolecular structure of cotton fiber is not significantly damaged by alkaline treatment and MCA grafting, while the density of the alkalized fabric is increased by 20% with respect to the raw fabric, so the breaking strength is obviously enhanced. After sodium periodate treatment, the tensile strength of cotton fabric is reduced by 36.1% because the C_2–C_3 bonds are fractured due to the selective oxidation of sodium periodate, damaging the original macromolecular structure of cotton fabric to a certain degree (Yue et al. 2014). The breaking strength of the fabric treated with L-Glu is further reduced, which is

Table 3 Whiteness and tensile properties of cotton fabric after each treatment step

Sample	Breaking strength (N)	Breaking elongation (mm)	Elongation (%)	Work of fracture (J)	Whiteness index (%)
COT	368.4 ± 24.2	22.59 ± 0.70	22.29 ± 0.69	0.46 ± 0.03	85.14
COT-M	433.2 ± 31.7	15.28 ± 0.51	15.08 ± 0.50	0.44 ± 0.05	82.27
COT-CMC	466.8 ± 26.8	34.69 ± 1.25	34.11 ± 1.18	0.87 ± 0.01	/
COT-DCMC	298.2 ± 20.0	20.83 ± 0.83	20.98 ± 0.84	0.41 ± 0.04	/
COT-Glu	308.4 ± 18.3	31.43 ± 1.18	31.86 ± 1.19	0.59 ± 0.02	/
COT-Glu–Ca	309.6 ± 17.6	32.63 ± 1.39	32.17 ± 1.37	0.64 ± 0.03	81.62

Fig. 9 Water contact angle images of cotton fabric before and after modification: COT (left) and COT-Glu–Ca (right)
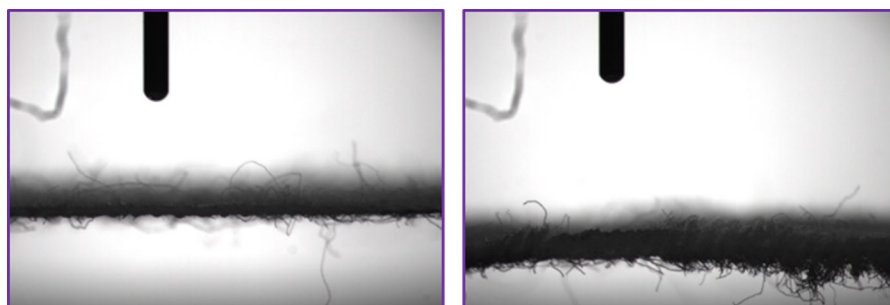
related to the acid resistance of cotton fabric. However, the strength of COT-Glu–Ca fabric is only slightly higher than that of COT-Glu because of the formation of intramolecular and intermolecular network structure between –COO- and Ca^{2+}, which results in hindered slippage between the macromolecular chains of fibers during the stretching process to some extent (Luo et al. 2020). In summary, the mechanical properties of fabrics after and before modification are almost the same, which meets the strength requirement in practical applications.

The whiteness of the control cotton sample is 85.14%, which decreases by just 3.37% and 2.96% after treatment with 24 wt% NaOH and $CaCl_2$, respectively, indicating that the whiteness of the cotton is effectively retained after treatment. In addition, the WG is tested, which exhibits an increase of 10.26% after modification.

According to the contact angle test (Fig. 9), the water contact angle of cotton fabric is 0°, showing excellent hydrophilicity, which remains the same after modification (COT-Glu–Ca). The wetting time of both original cotton fabric and flame-retardant fabric is approximately 1 s, indicating that the wettability of the fabric remains almost unchanged after flame-retardant modification. The above results further suggest that the chelation of calcium ions with –COO- endows the cotton fabric with excellent flame retardancy, while the other properties of the fabric are not affected.

Conclusions

A novel halogen-free flame-retardant cotton fabric that does not release formaldehyde during use and production is synthesized, which forms a unique skeleton network structure covering the surface and interior of cotton cellulose to enhance the connection between the macromolecules. This modification strategy dramatically improves the flame-retardant effect as well as the self-extinguishing property of cotton fabrics during combustion, whose LOI value is up to 33.6% and the char length is only 53 mm after 12 s of burning. The gases produced from thermal decomposition react with the chelated Ca^{2+} ions to prevent the transmission of heat, flame, and oxygen and to inhibit the internal fibers from thermal decomposition. The final cotton fabric not only exhibits outstanding fire retardancy but also retains whiteness, breaking strength, and good hygroscopicity. Overall, this work establishes an effective approach for the fabrication of flame-retardant cotton fabrics without halogen, phosphorus, and formaldehyde without altering their intrinsic properties.

Declarations

References

Abidi N, Cabrales L, Haigler CH (2014) Changes in the cell wall and cellulose content of developing cotton fibers investigated by FTIR spectroscopy. Carbohydr Polym 100:9–16. https://doi.org/10.1016/j.carbpol.2013.01.074

Agulhon P, Markova V, Robitzer M, Quignard F, Mineva T (2012) Structure of alginate gels: interaction of diuronate units with divalent cations from density functional calculations. Biomacromol 13(6):1899–1907. https://doi.org/10.1021/bm300420z

Castellano A, Colleoni C, Iacono G, Mezzi A, Plutino MR, Malucelli G et al (2019) Synthesis and characterization of a phosphorous/nitrogen based sol-gel coating as a novel halogen- and formaldehyde-free flame retardant finishing for cotton fabric. Polym Degrad Stab 162:148–159. https://doi.org/10.1016/j.polymdegradstab.2019.02.006

Chen HB, Wang YZ, Sánchez-Soto M, Schiraldi DA (2012) Low flammability, foam-like materials based on ammonium alginate and sodium montmorillonite clay. Polymer 53(25):5825–5831. https://doi.org/10.1016/j.polymer.2012.10.029

Chen Y, Liu SD, Wan CY, Zhang GX (2021) Facile synthesis of a high efficiency and durability L- citrulline flame retardant for cotton. Int J Biol Macromol 166:1429–1438. https://doi.org/10.1016/j.ijbiomac.2020.11.022

French AD (2014) Idealized powder diffraction patterns for cellulosepolymorphs. Cellulose 21:885–896. https://doi.org/10.1007/s10570-013-0030-4

French AD (2017) Glucose, not cellobiose, is the repeating unit of cellulose and why that is important. Cellulose 24(11):4605–4609. https://doi.org/10.1007/s10570-017-1450-3

Hong TZ, Lv ZH, Liu X, Li W, Nai XY, Dong YP (2016) A novel surface modification method for anhydrite whisker. Mater Des 107:117–122. https://doi.org/10.1016/j.matdes.2016.06.034

Hou XB, Xue ZX, Xia YZ (2018) Preparation of a novel agar/sodium alginate fire-retardancy film. Mater Lett 233:274–277. https://doi.org/10.1016/j.matlet.2018.09.026

Jin E, Guo JQ, Yang F, Zhu YY, Song JL, Jin YC, Rojas OJ (2016) On the polymorphic and morphological changes of cellulose nanocrystals (CNC-I) upon mercerization and conversion to CNC-II. Carbohydr Polym 143:327–335. https://doi.org/10.1016/j.carbpol.2016.01.048

Kabir II, Sorrell CC, Mofarah SS, Yang W, Yuen ACY, Nazir MT et al (2020) Alginate/polymer-based materials for fire retardancy: synthesis, structure, properties, and applications. Polym Rev 61(2):357–414. https://doi.org/10.1080/15583724.2020.1801726

Kafle K, Greeson K, Lee C, Kim SH (2014) Cellulose polymorphs and physical properties of cotton fabrics processed with commercial textile mills for mercerization and liquid ammonia treatments. Text Res J 84:1692–1699. https://doi.org/10.1177/0040517514527379

Kang HA, Shin MS, Yang JW (2002) Preparation and characterization of hydrophobically modified alginate. Polym Bull 47:429–435

Leal D, Matsuhiro B, Rossi M, Caruso F (2008) FT-IR spectra of alginic acid block fractions in three species of brown seaweeds. Carbohydr Res 343(2):308–316. https://doi.org/10.1016/j.carres.2007.10.016

Li JW, He JM, Huang YD, Li DL, Chen XT (2015) Improving surface and mechanical properties of alginate films by using ethanol as a co-solvent during external gelation. Carbohydr Polym 123:208–216. https://doi.org/10.1016/j.carbpol.2015.01.040

Li ZF, Zhang CJ, Cui L, Zhu P, Yan C, Liu Y (2017) Fire retardant and thermal degradation properties of cotton fabrics based on APTES and sodium phytate through layer-by-layer assembly. J Anal Appl Pyrolysis 123:216–223. https://doi.org/10.1016/j.jaap.2016.11.026

Lin DM, Zeng XR, Li HQ, Lai XJ, Wu TY (2019) One-pot fabrication of superhydrophobic and flame-retardant coatings on cotton fabrics via sol-gel reaction. J Colloid Interface Sci 533:198–206. https://doi.org/10.1016/j.jcis.2018.08.060

Liu Y, Zhao JC, Zhang CJ, Ji H, Zhu P (2014) The Flame retardancy, thermal properties, and degradation mechanism of zinc alginate films. J Macromol Sci Part B Phys 53(6):1074–1089. https://doi.org/10.1080/00222348.2014.891169

Liu WJ, Zhang SQ, Wang WQ, Zhang J, Yan W, Deng J et al (2015a) The effects of Ca(II) and Mg(II) ions on the flotation of spodumene using NaOL. Miner Eng 79:40–46. https://doi.org/10.1016/j.mineng.2015.05.008

Liu Y, Zhao JC, Zhang CJ, Guo Y, Zhu P, Wang DY (2015b) Effect of manganese and cobalt ions on flame retardancy and thermal degradation of bio-based alginate films. J Mater Sci 51(2):1052–1065. https://doi.org/10.1007/s10853-015-9435-9

Liu Y, Zhao XR, Peng YL, Wang D, Yang LW, Peng H et al (2016) Effect of reactive time on flame retardancy and thermal degradation behavior of bio-based zinc alginate film. Polym Degrad Stab 127:20–31. https://doi.org/10.1016/j.polymdegradstab.2015.12.024

Liu ZY, Xu MJ, Wang Q, Li B (2017) A novel durable flame retardant cotton fabric produced by surface chemical grafting of phosphorus- and nitrogen-containing compounds. Cellulose 24(9):4069–4081. https://doi.org/10.1007/s10570-017-1391-x

Liu YS, Zhao WJ, Yu X, Zhang JY, Ren YL, Liu XH et al (2022) Preparation of dyeing, flame retardant and anti-dripping polyethylene terephthalate fibers based on natural sodium copper chlorophyll dyeing and intercalation of phosphorylated sucrose fatty acid ester. Compos Part B-Eng 245:110194. https://doi.org/10.1016/j.compositesb.2022.110194

Lu Y, Jia YL, Zhang GX, Zhang FX (2018) An eco-friendly intumescent flame retardant with high efficiency and durability for cotton fabric. Cellulose 25(9):5389–5404. https://doi.org/10.1007/s10570-018-1930-0

Luo QL, Gao P, Zhou J, Zhang J, Wu W, Cao JD et al (2020) Imparting flame resistance to citric acid–modified cotton fabrics using DNA. J Eng Fibers Fabr 15:1–10. https://doi.org/10.1177/1558925020922217

Lv FB, Zhu P, Wang CX, Zheng LM (2012) Preparation, characterization, and dyeing properties of calcium alginate fibers. J Appl Polym Sci 126(S1):E383–E388. https://doi.org/10.1002/app.36673

Mendoza DJ, Browne C, Raghuwanshi VS, Simon GP, Garnier G (2019) One-shot TEMPO-periodate oxidation of native cellulose. Carbohydr Polym 226:115292. https://doi.org/10.1016/j.carbpol.2019.115292

Miao ZW, Yan DP, Zhang T, Yang F, Zhang SK, Liu W et al (2021) High-efficiency flame retardants of a P-N-Rich Polyphosphazene Elastomer Nanocoating on Cotton Fabric. ACS Appl Mater Interfaces 13(27):32094–32105. https://doi.org/10.1021/acsami.1c05884

Pinto RJB, Neves MC, Neto CP, Trindade T (2012) Growth and chemical stability of copper nanostructures on cellulosic fibers. Eur J Inorg Chem 2012:5043–5049. https://doi.org/10.1002/ejic.201200605

Qu HQ, Liu YS, Zhao WJ, Zhang JY, Ren YL, Liu XH (2022) Inspired by sodium alginate: amino acids cooperating with sodium ions to prepare phosphorus-free flame retardant lyocell fabric. Cellulose 29:5339–5358. https://doi.org/10.1007/s10570-022-04596-5

Rosace G, Colleoni C, Trovato V, Iacono G, Malucelli G (2017) Vinylphosphonic acid/methacrylamide system as a durable intumescent flame retardant for cotton fabric. Cellulose 24(7):3095–3108. https://doi.org/10.1007/s10570-017-1294-x

Shariatinia Z, Javeri N, Shekarriz S (2015) Flame retardant cotton fibers produced using novel synthesized halogen-free phosphoramide nanoparticles. Carbohydr Polym 118:183–198. https://doi.org/10.1016/j.carbpol.2014.11.039

Tian JL, Yu WH, Pan J, Wang K, Qi ZM, Lin L et al (2022) Synthesis of reactive flame retardant containing Si–P–S–N and its application in cotton fabric. Cellulose 30(4):2551–2572. https://doi.org/10.1007/s10570-022-04991-y

Wang AW, Zhu Q, Xing ZP (2019a) A functionalized chitosan wrinkled hollow sphere containing calcium ions: Efficient adsorption of sodium dodecylbenzenesulfonate (SDBS) from aqueous solutions. J Colloid Interface Sci 555:203–213. https://doi.org/10.1016/j.jcis.2019.07.086

Wang YF, Khoso SA, Luo XM, Tian MJ (2019b) Understanding the depression mechanism of citric acid in sodium oleate flotation of Ca^{2+}-activated quartz: experimental and DFT study. Miner Eng 140:105878. https://doi.org/10.1016/j.mineng.2019.105878

Wei GL, Li DQ, Zhuo MN, Liao YS, Xie ZY, Guo TL et al (2015) Organophosphorus flame retardants and plasticizers: sources, occurrence, toxicity and human exposure. Environ Pollut 196:29–46. https://doi.org/10.1016/j.envpol.2014.09.012

Xiao YL, Ma C, Jin ZY, Wang JL, He LX, Mu XW et al (2021) Functional covalent organic framework for exceptional Fe^{2+}, Co^{2+} and Ni^{2+} removal: an upcycling strategy to achieve water decontamination and reutilization as smoke suppressant and flame retardant simultaneously. Chem Eng J 421:127837. https://doi.org/10.1016/j.cej.2020.127837

Xing LD, Hu CS, Zhang WW, Guan LT, Gu J (2020) Transition of cellulose supramolecular structure during concentrated acid treatment and its implication for cellulose nanocrystal yield. Carbohydr Polym 229:115539. https://doi.org/10.1016/j.carbpol.2019.115539

Yang JW, Zhao WJ, Li Y (2021) Human health risk regulation of reproductive toxicity, neurotoxicity, and endocrine disruption in special populations exposed to organophosphorus flame retardants. Exposure and Health 13(3):551–566. https://doi.org/10.1007/s12403-021-00402-y

Yue XX, Lin HT, Yan T, Zhang DS, Lin H, Chen YY (2014) Synthesis of silver nanoparticles with sericin and functional finishing to cotton fabrics. Fibers and Polymers 15(4):716–722. https://doi.org/10.1007/s12221-014-0716-8

Zhang JJ, Ji Q, Wang FJ, Tan LW, Xia YZ (2012) Effects of divalent metal ions on the flame retardancy and pyrolysis products of alginate fibres. Polym Degrad Stab 97(6):1034–1040. https://doi.org/10.1016/j.polymdegradstab.2012.03.004

Zhang YF, Zhang LL, Shao SJ, Chang XL, Li M (2020) Periodate oxidation of carboxymethyl cellulose under controlled conditions. ChemistrySelect 5(22):6765–6773. https://doi.org/10.1002/slct.202000470

Zhang AN, Zhao HB, Cheng JB, Li ME, Li SL, Cao M et al (2021) Construction of durable eco-friendly biomass-based flame-retardant coating for cotton fabrics. Chem Eng J 410:128361. https://doi.org/10.1016/j.cej.2020.128361

Zhang Y, Li TT, Shiu BC, Lin JH, Lou CW (2022) Multifunctional sodium Alginate@ urushiol fiber with targeted Antibacterial, acid corrosion resistance and flame retardant properties for personal protection based on wet spinning. Appl Surf Sci 584:152573. https://doi.org/10.1016/j.apsusc.2022.152573